Symplectic structure and monopole strength in ^{12}C

T. Yoshida
Center for Nuclear Study, Graduate School of Science, University of Tokyo, 7-3-1 Hongo, 133-0033 Tokyo, Japan

N. Itagaki
Yukawa Institute for Theoretical Physics, Kyoto University, Kitashirakawa Oiwake-Cho, 606-8502 Kyoto, Japan

K. Katō
Department of Physics, Faculty of Science, Hokkaido University, Kita 10 Nishi 8, 060-0810 Sapporo, Japan
(Received 13 October 2010; revised manuscript received 1 December 2010; published 1 February 2011)

The relation between the monopole transition strength and existence of cluster structure in the excited states is discussed based on an algebraic cluster model. The structure of ^{12}C is studied with a 3α model, and the wave function for the relative motions between α clusters are described by the symplectic algebra $\mathrm{Sp}(2,R)_z$, which corresponds to the linear combinations of SU(3) states with different multiplicities. Introducing $\mathrm{Sp}(2,R)_z$ algebra works well for reducing the number of the basis states, and it is also shown that states connected by the strong monopole transition are classified by a quantum number Λ of the $\mathrm{Sp}(2,R)_z$ algebra.

DOI: 10.1103/PhysRevC.83.024301 PACS number(s): 21.10.−k, 21.60.Gx, 27.20.+n

I. INTRODUCTION

Light nuclear systems show many different properties in the structure. Around the low-lying energy region, the mean field and the associated shell structure are dominant properties, however, cluster structures appear close to their decay thresholds. In this context, an α particle that is strongly bound and an α-α interaction that is not strong enough to make a bound state, can be considered as an effective building block of the structure of light nuclei [1]. One of the typical examples of cluster structures is the second 0^+ (0^+_2) state of ^{12}C at $E_x = 7.65$ MeV just above the 3α-threshold energy. This state is considered to have an exotic cluster structure of 3α in analogy with the so-called "mysterious 0^+ state" of ^{16}O at $E_x = 6.06$ MeV, which has a $^{12}\mathrm{C} + \alpha$ cluster structure and is hardly explained by a simple shell-model picture. The 0^+_2 state plays a crucial role in synthesis of ^{12}C from three ^{4}He nuclei in stars [2], and the state was proven to contain a developed 3α configuration by many microscopic cluster calculations [3,4], which is a gaslike state without a specific geometrical shape. This state is recently reinterpreted as an α-condensed state [5–7].

To prove the existence of cluster states, recently it was proposed that the strong enhancement of isoscalar monopole ($E0$) transitions can be a measure of the cluster structure [8]. For instance, the presence of the cluster states in ^{13}C was suggested by measuring the isoscalar $E0$ transitions from the ground $1/2^-$ state induced by the $^{13}\mathrm{C}(\alpha,\alpha')^{13}\mathrm{C}$ reaction [9]. The obtained cross sections are much larger than those of the shell-model calculations, which suggests that protons and neutrons are coherently excited and they have spatially extended distribution in the excited states.

From the theoretical side, the relation between the monopole transition strength and the cluster structure was also discussed [10–13]. The basic idea arises from the Bayman-Bohr theorem [14], which shows that the lowest representation of the shell model contains a component of the lowest SU(3) representation of the cluster states. Thus, even cluster states with spatially extended distribution, such as the second 0^+ state of ^{12}C, can be generated by multiplying operators to the shell-model-like ground state. The monopole operator is the very one that induces the spatial extension of the ground state and connects it to cluster states by raising the quanta of the cluster-cluster relative wave function by two. The monopole matrix element of $^{12}\mathrm{C}$ ($0^+_1 \to 0^+_2$) calculated with the cluster model agrees with the experimental value (5.4 ± 0.2 fm^2 for proton part [15]), and this is much larger than that given in the p-shell single-particle models. This is one of the supports for the proposal that a strong monopole transition can be a signature of $4N$ correlated states from the theoretical side. It is also discussed that the mixing of the cluster component in the ground state is another important factor for the enhancement of the monopole transition strength to cluster states [13].

In the present study, the relation between the monopole transition strength and the existence of a well-developed cluster structure in the excited states is discussed based on an algebraic cluster model. The structure of ^{12}C is studied with a 3α model, and the wave functions for the relative motions between α clusters are described by the harmonic oscillator (HO) basis states forming symplectic algebra. The importance of the symplectic structure for light nuclei was also investigated in Refs. [16,17], and the relation between the symplectic algebra and the cluster model was discussed. In our study, we focus on the relation between the symplectic structure and monopole transition strength. As a final goal of this study, we aim to treat the solution of the unbound states in a correct way and explicitly impose the boundary conditions in the outer region. For this purpose, it is necessary to introduce basis states with large principal quantum numbers for the relative motion of clusters, but the number of the basis states drastically increases with increasing principal quantum numbers if we adopt SU(3) algebra.

This problem is overcome by introducing symplectic algebra $\mathrm{Sp}(2,R)_z$, where the basis states correspond to the linear combinations of SU(3) states with different multiplicities. This $\mathrm{Sp}(2,R)_z$ algebra can be a powerful tool to create the states corresponding to the excitation modes of relative motions between α clusters. The cluster states with SU(3) representations that have different total HO quanta are connected by a common eigenvalue Λ of the $\mathrm{Sp}(2,R)_z$ algebra, and it will be shown that strong monopole transitions are classified by this Λ. It is also discussed that limited values (small values) of Λ are enough to achieve good convergence for the states corresponding to the excitation modes of the clusters [18]. Because of this effect, we can adopt states with large values of the HO quanta into the model space in this study.

The outline of this paper is given as follows. Firstly, we show the framework of the symplectic model in Sec. II. In Sec. III, we calculate the energy and the monopole transition strength of ^{12}C. Here, we discuss the relation between the symplectic quanta Λ and the monopole transition strength. We summarize the discussion in Sec. IV.

II. $\mathrm{SP}(2,R)_z$ BASIS REPRESENTATION OF THE 3α MODEL

We show how to construct a model space of the 3α system based on the SU(3) algebra. However, the $\mathrm{Sp}(2,R)_z$ algebra, which corresponds to the linear combination of SU(3) basis states with different multiplicities, is shown to give better description for the cluster states. The relation between the SU(3) and $\mathrm{Sp}(2,R)_z$ model spaces is discussed.

A. SU(3) model space

Here, we show how to construct basis states of the 3α-cluster system based on the SU(3) algebra. The SU(3) state of the three-α cluster model for ^{12}C is given by a product of SU(3) states corresponding to the two Jacobi coordinates for the relative motions of α-α ($\vec{r}$) and (α-α)-α ($\vec{R}$):

$$\mathrm{SU(3)} = \mathrm{SU(3)} \otimes \mathrm{SU(3)}. \tag{1}$$

Using the $(\lambda,\mu)\rho$ representation of SU(3), the basis state with the principal HO quantum numbers N is expressed as

$$N(\lambda,\mu)\rho \sim (N_1,0) \otimes (N_2,0), \tag{2}$$

where N_1 and N_2 are principal HO quantum numbers ($N = N_1 + N_2$) for the Jacobi coordinates ($\vec{r}$ and $\vec{R}$) and ρ is the multiplicity of the (λ,μ) state. Following Refs. [19,20], the basis function with the values of $N(\lambda,\mu)\rho$, N_1, N_2, J, and K is given as

$$V^{N(\lambda,\mu),J,K}_{N_1,N_2}(\vec{r},\vec{R}) = \sum_{l_1,l_2} \langle (N_1,0), l_1, (N_2,0), l_2 || N(\lambda,\mu), J, K \rangle \times \left[u_{N_1,l_1}(\vec{r}) u_{N_2,l_2}(\vec{R}) \right]_J, \tag{3}$$

where l_1 and l_2 are angular momenta of each Jacobi coordinate, J is the total angular momentum, and K is the orthonormalized K-quantum number of J. We take summation over N_1 and N_2 in the following way:

$$U_i^{J^\pi}(\vec{r},\vec{R}) = \sum_{N_1+N_2=N} A^{N(\lambda,\mu)\rho}_{N_1,N_2} V^{N(\lambda,\mu),J,K}_{N_1,N_2}(r,R), \tag{4}$$

where the index i denotes an abbreviation of $N(\lambda,\mu)\rho, K$. To take into account the Pauli principle between nucleons belonging to different α clusters, the coefficients $A^{N(\lambda,\mu)\rho}_{N_1,N_2}$ must be determined by the orthogonal condition model (OCM) [21,22]. First of all, the value of N_1 should be the Pauli-allowed one ($N_1 = 4, 6, 8, \ldots, N$). For N_2, instead of directly calculating the Pauli-allowed state for the Jacobi coordinate $\vec{R}$ [23], here we calculate the overlap with the Pauli-forbidden state of rearranged Jacobi coordinates. Eventually, the Pauli-allowed basis states for Jacobi coordinates $(\vec{r},\vec{R})$ are obtained by orthogonalizing the basis states to the Pauli-forbidden ones with other (rearranged) sets of Jacobi coordinates $(\vec{r}',\vec{R}')$ and $(\vec{r}'',\vec{R}'')$. Here, it is enough if we only consider the Pauli-forbidden states for the coordinates $\vec{r}'$ and $\vec{r}''$, which have the principal quantum number of $N_1', N_1'' = 0, 1, 2, 3, 5, 7, 9, \ldots$. This is equivalent to the following condition [24]:

$$\hat{Q}|N(\lambda,\mu)k\rangle = q_k|N(\lambda,\mu)k\rangle. \tag{5}$$

Here, the operator $\hat{Q}$ expresses the projection to the Pauli-forbidden states for all different Jacobi coordinates, and the Pauli-allowed states are obtained as the eigenstates of $q_k = 0$, because they have to be orthogonal to all the Pauli-forbidden states. The index k is needed to distinguish the multiplicity of the wave function, which has a set of the HO quanta of N_1 and N_2. The wave function of the 3α model for ^{12}C is constructed by superposing $U_i(\vec{r},\vec{R})$ basis states. The size of the model space is determined by the maximum HO quanta $N_{\max}$ as follows:

$$\Phi^{J^\pi} = \sum_{i=N(\lambda,\mu)\rho,K} c_i^{J^\pi} U_i^{J^\pi}(\vec{r},\vec{R}), \tag{6}$$

where the summation runs under the condition $N \leqslant N_{\max}$.

B. Hamiltonian

The Hamiltonian H is given in the following form:

$$H = T_{\vec{r}} + T_{\vec{R}} + \sum_{i>j} V_{\alpha\alpha}(\vec{r_{ij}}) + V^J_{3by}(\vec{r}_1,\vec{r}_2,\vec{r}_3), \tag{7}$$

where $T_{\vec{r}}$ and $T_{\vec{R}}$ are relative kinetic energies corresponding to the Jacobi coordinates. As for the two-body nuclear interaction, we use the following α-α folding potential:

$$V_{\alpha\alpha}(r) = V_2 \exp(-\alpha r^2), \tag{8}$$

employed by Kurokawa *et al*. so as to reproduce the observed α-α phase shifts [25,26]. Here, $\alpha = 0.2009$ fm^{-2} and $V_2 = -106.1$ MeV are used. The Coulomb interaction has the following form:

$$V_c^{\alpha\alpha}(r) = \frac{4e^2}{r}\mathrm{erf}(\beta r), \tag{9}$$

where $\beta = 0.5972$ fm^{-1}. Moreover, we add an inter three-α interaction:

$$V^J_{3by}(\vec{r}_1,\vec{r}_2,\vec{r}_3) = V_3^J \exp\left(-\eta\left\{r_{12}^2 + r_{23}^2 + r_{31}^2\right\}\right), \tag{10}$$

where $\eta = 0.15$ fm^{-2} and $r_{ij} = r_i - r_j$. To reproduce the experimental binding and excitation energies of the ground

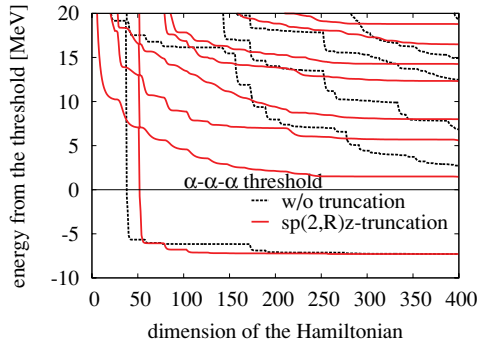

FIG. 1. (Color online) Energy convergence of the 3α system as a function of the number of basis states. The black (dashed) and red (solid) lines show the results for the SU(3) and $\mathrm{Sp}(2,R)_z$ basis sets, respectively.

band states (0^+, 2^+ and 4^+) of ^{12}C [26], we need to use the strength of the three-body interaction V_3^J as, 31.7 MeV for $J=0^+$, 63.0 MeV for $J=2^+$, and 150.0 MeV for $J=4^+$, respectively.

Energies and their eigenstates [Eq. (6)] are obtained by diagonalization of the Hamiltonian [Eq. (7)]. In Fig. 1, we show the convergence of the 0^+ states as a function of the number of basis states (black dotted lines), where $N_{\max}$ is gradually increased from 8 to 46 in the SU(3) basis. It is shown that the ground states has rapid convergence, which indicates the importance of the shell-model-like configuration. On the other hand, many excited states show slow convergence, which means that the SU(3) model space is not suitable for the description of the well-developed cluster states in the excited states. This is because of the increase of multiplicity useless for the convergence as the total HO quanta N increases.

C. $\mathrm{Sp}(2,R)_z$ model space

To achieve the energy convergence in a more efficient way especially for the cluster states in the excited states, we need appropriate truncation for the model space. To describe the cluster-like configuration, we take into account the major-shell excitation including many HO N-quanta states. Here, we intend to correlate different N-quanta states by algebraic classifications. We perform unitary transformation of the states specified by ρ to the other basis sets by utilizing the N_1 and N_2 degrees of freedom. Here, we use the symplectic algebra, $\mathrm{Sp}(2,R)_z$. According to this algebra, basis states are classified by a quantum number Λ, which is an eigenvalue of the Casimir operator of this algebra [18]. This Λ specifies the ladder states; a set of ladder states has definite eigenvalue of Λ. The generators of this algebra are given as

$$\begin{aligned}\Lambda_+ &= \frac{1}{\sqrt{8}}\sum_{p=1}^{2} a_z^\dagger(p)a_z^\dagger(p),\\ \Lambda_- &= -\frac{1}{\sqrt{8}}\sum_{p=1}^{2} a_z(p)a_z(p),\\ \Lambda_0 &= \frac{1}{4}\sum_{p=1}^{2}(a_z^\dagger(p)a_z(p)+a_z(p)a_z^\dagger(p)).\end{aligned} \tag{11}$$

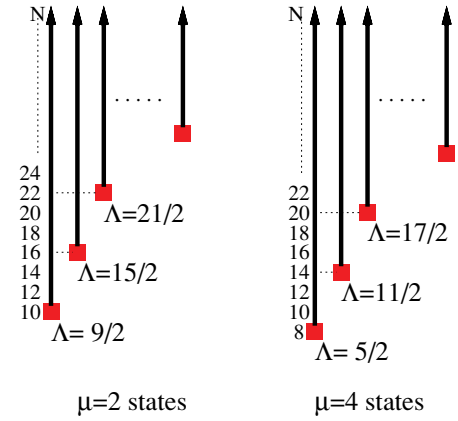

FIG. 2. (Color online) Pauli-allowed states generated by $\mathrm{Sp}(2,R)z$ algebra. The red squares, vertical lines, and arrows show the band head state, the principal quantum number N of HO, and the ladder states, respectively.

Here, $a_z^\dagger(p)$ and $a_z(p)$ are creation and annihilation operator of HO, respectively, where p is an index to distinguish the Jacobi coordinates $\vec{r}$ and $\vec{R}$. By using these operators, the ladder states are created by multiplying a raising operators Λ_+ to the band head state, which vanishes when a lowering operator Λ_- is multiplied. Note that each ladder state has a definite eigenvalue of Λ, and multiplying Λ_+ and Λ_- does not change this value. As shown in Fig. 2, a new band head state appears when the principal quantum number of HO (N) increases by six for each μ state [$N=\lambda+2\mu$, $\Lambda=\frac{1}{2}(\lambda+\mu)+\frac{1}{4}(n-1)$, where n is an integer]. However, we need to orthonormalize them by the Gram-Schmidt's procedure, because these new band states are not always orthogonal to the band states which have smaller Λ values.

To select the model space suited for the description of the excited states, we use of the limited Λ values. The truncated model space is expanded by the following basis states as

$$w_\alpha^{J^\pi}(\vec{r},\vec{R}) = \sum_\rho C_\rho^\Lambda U_i^{J^\pi}(\vec{r},\vec{R}), \tag{12}$$

where the index α denotes an abbreviation of Λ and $N(\lambda,\mu)$. The equation to be solved is expressed as

$$\sum_\beta H_{\alpha,\beta} d_{k,\beta}^{J^\pi} = E d_{k,\alpha}^{J^\pi}, \tag{13}$$

where the matrix element of the Hamiltonian is expressed as

$$H_{\alpha,\beta} = \langle w_\alpha | H | w_\beta \rangle. \tag{14}$$

The total wave function of the kth state is expressed as

$$\Phi^{J^\pi}(k) = \sum_\alpha d_{k,\alpha}^{J^\pi} w_\alpha^{J^\pi}(\vec{r},\vec{R}). \tag{15}$$

We employ this $w_\alpha^{J^\pi}$ basis set, which is of the $\mathrm{Sp}(2,R)_z$ truncation, and shown as the red solid lines of Fig. 1, the energy convergence becomes much faster compared with the case without this truncation (black dotted lines), especially for the excited states with well-developed cluster configurations. This good energy convergence can be obtained even if we limit Λ values. Here, we use the three lowest Λ values for each

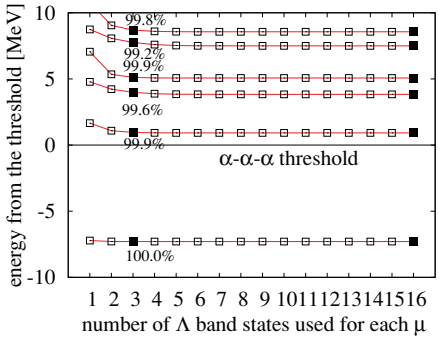

FIG. 3. (Color online) Energy convergence of the 0^+ states of the 3α system as a function of the size of the model space (the number of Λ band states included in the model space for each μ state). The left solid dots show the model space used in the present calculation, whereas the right solid dots show the model space with all Λ configurations. The numbers are overlaps with these two wave functions.

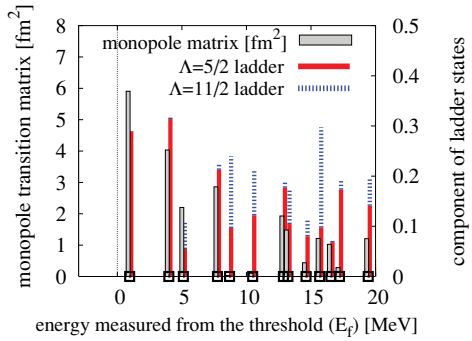

FIG. 4. (Color online) The relation between the monopole matrix from the ground state (left vertical axis) and components of ladder states of $\mathrm{Sp}(2,R)_z$ algebra (right vertical axis) for each 0^+ state. The squares show the eigenvalues of the Hamiltonian within the bound state approximation.

μ state. In return, we take total HO quanta $N_{\max} = 100$ and the μ values up to 30, which is difficult to achieve in the SU(3) case. This gives a model space large enough to describe the cluster states. To confirm the validity of the selection of Λ values, we show the energy convergence of the 0^+ states of the 3α system as a function of the size of the model space (the number of Λ band states included in the model space for each μ state) in Fig. 3. We find that the model space within the three lowest Λ values for each μ state already has enough good convergence (solid points) at this energy region. Moreover, the overlaps between these states and the full Λ band calculation (right solid points) are almost 100%. Therefore, we use this truncated model space in the present calculation.

III. RESULTS

A. Relation between monopole transitions and $\mathrm{Sp}(2,R)_z$ algebra

Hereafter we employ a model space in the $\mathrm{Sp}(2,R)_z$ representation and discuss the relation between the symplectic ladder states and the monopole strengths. Because the ladder states are created by the operator Λ_+ ($= \frac{1}{\sqrt{8}} \sum_{p=1}^{2} a_z^\dagger(p) a_z^\dagger(p)$), it is considered that they have a strong relation with the monopole transition, which is excited by the operator $\hat{E}0 \propto r^2 + \frac{4}{3}R^2$ with the similar form.

Firstly, we show the ground-state properties obtained within the present model space. The calculated ground state contains the component of the lowest Pauli-allowed SU(3) representation $[(\lambda,\mu) = (0,4)]$ by 66%. However, the $\mathrm{Sp}(2,R)_z$ representation can be a better description; the squared overlap between the ground state and the $\Lambda = 5/2$ state, whose band head is $(\lambda,\mu) = (0,4)$, is 93%.

Next, we discuss the monopole transition matrix element (proton part) from the ground state to excited states with the energies of E_f measured from the threshold as shown in Fig. 4 (left vertical axis). The obtained value of $\sim$5.9 fm^2 to the second 0^+ state just above the threshold energy (calculated as $E_f = 0.96$ MeV) shows good agreement with the experimental value (5.4 ± 0.2 fm^2). Furthermore, we find correlation between the monopole transition strength and a Λ component in each excited state (right vertical axis of Fig. 4).

Here, $\Lambda = 5/2$ (red) and $11/2$ (blue) specify the components of the lowest and the second ladder states for $\mu = 4$ in each excited state. From this figure, we can find that the excited states that have large monopole strengths dominantly contain components of ladder states with the same Λ value as the ground state (5/2). On the other hand, we can see the tendency that the monopole matrix becomes small when the excited states dominantly have the components of higher ladder states such as $\Lambda = 11/2$. This is one clue to understand the correlation between the Λ value of the excited states and the monopole transition strength from the ground state.

To understand the previously mentioned behavior of the monopole transition with respect to Λ, we expand the monopole matrix $E0(0_1^+ \to 0_k^+)$ as

$$E0(0_1^+ \to 0_k^+) = \langle \Phi^{0^+}(k) | \hat{E}0 | \Phi^{0^+}(gs) \rangle = \sum_\alpha d_{k,\alpha}^{0^+} \langle w_\alpha^{0^+} | \hat{E}0 | \Phi^{0^+}(gs) \rangle, \quad (16)$$

where α again shows an abbreviation of $N(\lambda,\mu)\Lambda$. At first, we take notice on the matrix element $M_\alpha \equiv \langle w_\alpha^{0^+} | \hat{E}0 | \Phi^{0^+}(gs) \rangle$. In Fig. 5, the contribution of each $\mathrm{Sp}(2,R)_z$ basis state for M_α is shown.

For a given μ, the contribution of ladder states with the smallest Λ values are shown: $(\mu,\Lambda) = (0,13/2)$ (red), (2,9/2) (green), (4,5/2) (blue), (6,7/2) (purple), and (4,11/2) (sky blue). We find that $(\mu,\Lambda) = (2,13/2,$ (4,5/2), and (6,7/2) states have large contribution for M_α. The main reason comes from the fact that the monopole operator carries only two quanta and components of the ground state are concentrated in the $\Lambda = 5/2$ state. The contribution of other μ and Λ states, for example, $(\mu,\Lambda) = (0,13/2)$ (red line) and (4,11/2) (sky blue) are less than 1.0 fm^2 at each HO quanta N.

The overall behavior of the monopole transition strength is governed by this M_α value. However, the detail structure of $E0(0_1^+ \to 0_k^+)$ varies depending on the wave function of the

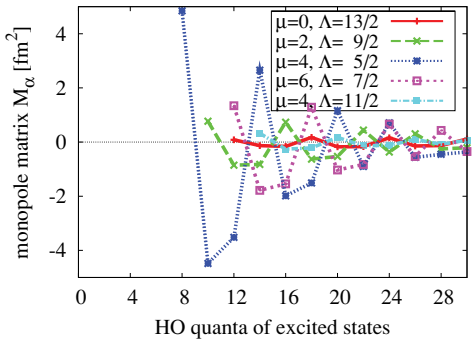

FIG. 5. (Color online) Decomposition of M_α in the contribution of each $Sp(2,R)_z$ basis state. For a given μ, contribution of ladder states with the smallest Λ values are shown: $(\mu,\Lambda) = (0,13/2)$ (red), (2,9/2) (green), (4,5/2) (blue), (6,7/2) (purple), and (4,11/2) (sky blue).

excited states. Therefore, next we discuss the relation between the matrix element M_α and the coefficients $d_{k,\alpha}$.

In Fig. 6, we depict the wave function of the second 0^+ state (calculated at $E_f = 0.96$ MeV) and monopole strength from the ground state. The following values, $\sum_\mu |d_{k,\alpha}|^2$ (light blue bars) and $|d_{k,\alpha_0}|^2$ (light blue bars) are shown in Fig. 6(a), whereas $d_{k,\alpha}M_\alpha$ (blue bars), $d_{k,\alpha_0}M_{\alpha_0}$ (red bars), and $|M_{\alpha_0}|$ (dot-dashed purple line) are shown in Fig. 6(b). Here, α_0 shows an abbreviation of $N(\lambda,\mu)\Lambda = N(\lambda,4)5/2$ quanta. Because the small Λ states are found to be important (in Fig. 5), here Λ (in α and α_0) is set to be the smallest for a given μ.

From this figure, we can see which part of the wave function is important for the monopole transition strength. For example, the HO quanta N of the second 0^+ state ($E_f = 0.96$ MeV) ranges up to $N \sim 60$ [Fig. 6 (a)]. The important N values can be determined by $d_{k,\alpha}M_\alpha$ (red and blue bars) value, which shows that the HO quanta up to $N \sim 40$ coherently contribute to the monopole value [Fig. 6(b)].

We can also investigate the transition to even higher excited states. The transition to the 0^+ state at $E_f = 5.12$ MeV is analyzed in Figs. 7(a) and 7(b) . This state has only small contribution of the α_0 state (light red bars). Even in such case, the small contributions of $d_{k,\alpha}M_\alpha$ (light blue bars) create a certain amount of the monopole matrix when they are summed over the HO quanta N, which is similar to the case of the second 0^+ state. The $d_{k,\alpha_0}M_{\alpha_0}$ value (red bars) and $\sum_\mu d_{k,\alpha}M_\alpha$ (blue bars) almost overlap with each other, which suggests the importance of the α_0 configuration $[N(\lambda,\mu)\Lambda) = N(\lambda,4)5/2]$ for the monopole transition strength.

In some of the excited states ($E_f = 3.99, 7.76, 8.69, 10.48, 12.86, 14.61, 15.67, 16.54, 17.21$, and 19.43 MeV), the slope of wave function strongly depends on the HO quanta N. As shown in Figs. 8(a) and 8(b) , the wave function of the 0^+ state at $E_f = 17.21$ (MeV) has clear nodes (light red bars) and they cause cancellation of the monopole strength (red bars). Therefore, the resultant monopole matrix becomes small. The transition to the states at the energies of $E_f = 8.69$, 10.48, 14.61, 15.67, and 19.43 MeV from the threshold also shows similar behavior (see Fig. 4). These states are related to the continuum solution, which will be discussed in the next subsection.

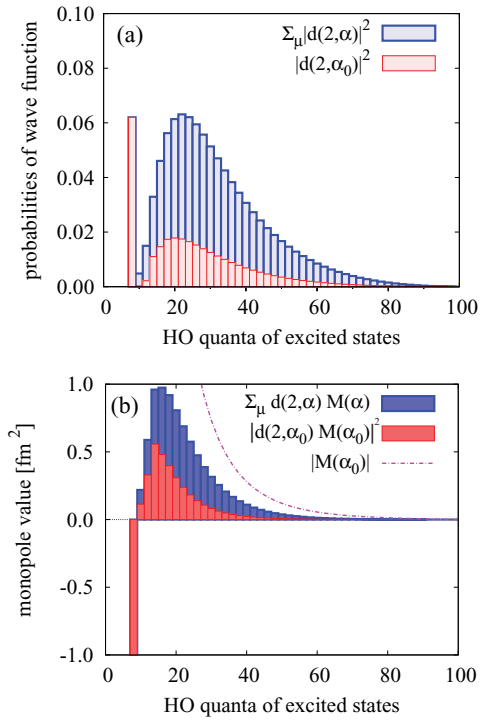

FIG. 6. (Color online) The relation between the wave function and monopole matrix for the second 0^+ state ($E_f = 0.96$ MeV) with respect to HO quanta N. In the upper panel (a), the light red box shows the component of wave function. The light blue box shows $\sum_\mu |d_{2,\alpha}|^2$, and the solid one shows the component of $|d_{2,\alpha_0}|^2$, where α_0 stands for $(\mu,\Lambda) = (4,5/2)$. In the lower panel (b), the red and blue box show M_α value multiplied by the coefficient of the wave function. The blue box shows $\sum_\mu d_{2,\alpha}M_\alpha$, and red one shows the component of $d_{2,\alpha_0}M_{\alpha_0}$. The dot-dashed purple line shows the $|M_{\alpha_0}|$ value. Here, α_0 shows an abbreviation of $N(\lambda,\mu)\Lambda = N(\lambda,4)5/2$ quanta.

We notice that N distributions of wave functions are also calculated by the Fermionic molecular dynamics (FMD) method [7]. The difference between the peak position of the second 0^+ states of ^{12}C in N (principal quantum number) between the present result and FMD comes from the definition of N. Our definition is the total principal quantum number, whereas the FMD one is the excitation of principal quantum number from the lowest shell-model state ($N = 8$). If we take into account this shift from the difference of the definition of N, both results are quite consistent. Our peak for the second 0^+ state around $N = 20$ corresponds to the peak around $N = 16$ in FMD. The state at $E_f = 3.99$ MeV has double peaks around $N = 16$ and $N = 58$. In the FMD calculation, such double-peak structure appears for the third 0^+ state (around $N = 14$–16 and 52–54).

B. Energy levels and properties of each state

In the last subsection, we discussed there is a tendency that states with components of lowest Λ are mainly excited when the monopole operator acts to the ground state. From this analysis, we can confirm the close relation between the symplectic structure and the monopole strength. However,

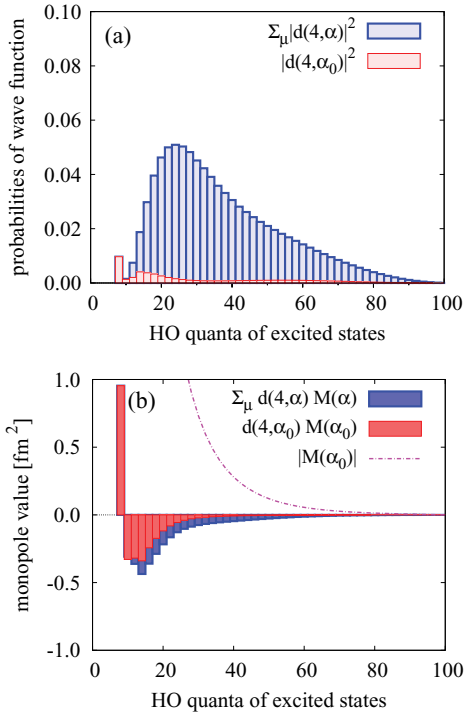

FIG. 7. (Color online) The same analyses as Fig. 6 for the 0^+ state at $E_f = 5.12$ MeV.

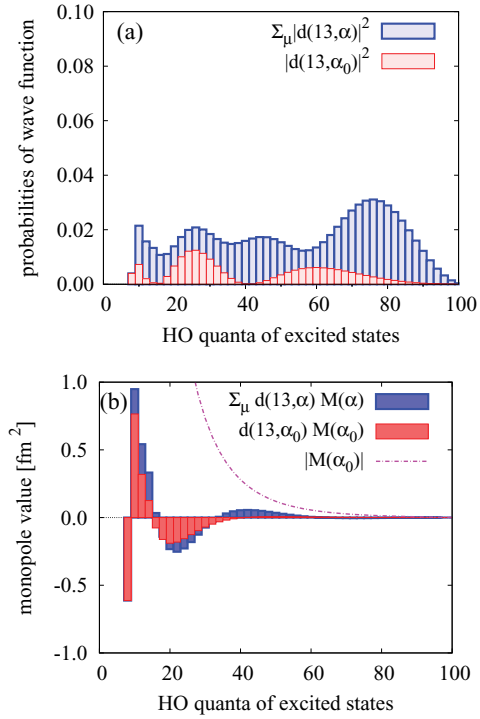

FIG. 8. (Color online) The same analyses as Fig. 6 for the 0^+ state at E_f =17.21 MeV.

we must keep in mind that not all of the states that have large monopole transitions survive as resonance states when we impose the correct boundary condition. The extraction of the resonance solution can be performed by drawing energy convergence with respect to the increase of the maximum HO quanta of the model space, $N_{\max}$. As shown in Fig. 9, the obtained states show the behavior of quasistationary solution at the energies of $E_f = 0.96$, 5.12, and 14.00 MeV from the threshold. These states are candidates for the resonance states. This is consistent with the previous work in Ref. [26].

TABLE I. Properties of ^{12}C levels. The root mean square radius [$R_{\text{r.m.s.}}$ (fm)] and squared overlap of each state with (μ,Λ) configuration (right column). The states with the parentheses (J^π) are obtained as bound state approximation but do not show the behavior of stationary solutions.

			(μ,Λ)		
E (MeV)	J^π	$R_{\text{r.m.s.}}$ (fm)	(0,13/2)	(2,9/2)	(4,5/2)
−7.29	0^+	2.39	0.00	0.02	0.93
−3.00	2^+	2.45	0.00	0.03	0.91
6.57	4^+	2.82	0.02	0.05	0.80
0.96	0^+	3.61	0.17	0.21	0.29
2.73	2^+	3.95	0.26	0.22	0.22
5.17	(4^+)	4.28	0.26	0.20	0.22
5.12	0^+	3.92	0.45	0.07	0.05
7.13	2^+	4.29	0.30	0.09	0.15
8.19	(4^+)	4.30	0.32	0.10	0.12
9.83	(4^+)	4.63	0.25	0.12	0.14

The obtained candidates for the resonance states after this treatment are shown in Fig. 10 together with the bound states. The left and right spectra correspond to the experimental and theoretical ones, respectively. The location of the theoretical ground band levels (0^+, 2^+, and 4^+) are fitted to the experimental ones by adjusting the strength of the three-body interaction given in Eq. (10).

The excited 0^+, 2^+, and 4^+ states are calculated using the same strengths of the three-body interaction as those for the ground band states. We can see a reasonable agreement with the experiment levels the same as in the previous calculations [13,26]. Here, the dotted lines with the parentheses (J) show the levels that are obtained as bound state approximation but do not show the behavior of stationary solutions by the analysis of Fig. 9.

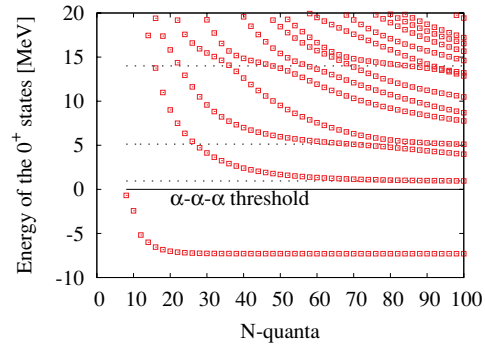

FIG. 9. (Color online) Energy convergence of the 3α system with respect to the increase of the N quanta for the model space ($N_{\max}$). The dotted line (black) shows the stationary points with respect to N, which are candidates for the resonance states.

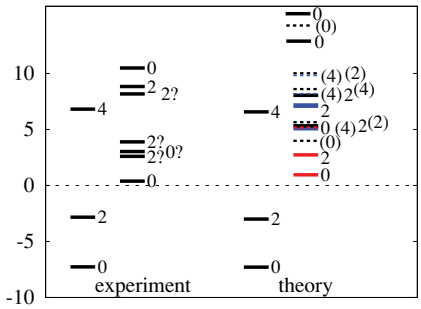

FIG. 10. (Color online) Energy spectra of ^{12}C (positive parity) measured from the threshold.

The property of each level is characterized by red and blue colors. Above the threshold, the red colored states, 0^+ (0.96 MeV), 2^+ (2.73 MeV), and 4^+ (5.17 MeV), have a gaslike nature of three α clusters, whereas the blue colored states, 0^+ (5.12 MeV), 2^+ (7.12 MeV), and 4^+ (8.19 and 9.83 MeV), have a considerable amount of linear-chain configurations.

These characters are deduced from the calculated root mean square radii ($R_{\text{r.m.s.}}$) and probabilities of each (μ,Λ) configuration listed in Table I. The gaslike states are characterized by the large $R_{\text{r.m.s.}}$ value, and because the wave function is dilutely distributed, it has components of various (μ,Λ) configurations. For instance, the 2_2^+ state ($E_f = 2.73$ MeV) is considered to have the gaslike nature. Although a candidate was reported [27], the excited states of the Hoyle state have not been experimentally confirmed.

On the other hand, the linear-chain states are characterized by large overlap with $\mu = 0$ configurations. The 0^+ state at $E_f = 5.12$ MeV obtained within the present framework contains the characteristics of linear-chain configuration. We can see that the amount of the linear-chain component decreases as J increases. Moreover, the stationary point of energy convergence indicates that the linear-chain structures tend to have relatively larger decay widths than the gaslike states. Therefore, the clear rotational band structure cannot be seen in the present calculation.

IV. SUMMARY

In this paper, we have studied the relation between the monopole transition strength of ^{12}C and the special algebraic structure to investigate the large strength including the one for ^{12}C ($0_1^+ \to 0_2^+$). Here, we have focused on the similarity of the monopole operator and the generators of the $\mathrm{Sp}(2,R)_z$ algebra. The model space is constructed based on the $\mathrm{Sp}(2,R)_z$ algebra, and the ladder states were generated from the band head states given by the SU(3) representation.

We have found that the large contribution for the monopole transition strength can be explained from the properties of the generators of $\mathrm{Sp}(2,R)_z$ and the ground state. We have been able to discuss the mechanism that the monopole strengths are closely related to the Λ value of the final states. Here, the importance of the Λ ladder state, which is the same as the ground state (α_0), was discussed. We found that the overall behavior of the monopole strength is given by the amount of α_0 configuration. However, the detailed value is sensitive to the properties of the wave function, where we have seen these values as a function of the N quanta of the harmonic oscillator. We have also seen that the mechanism appears even in the linear-chain-like 0^+ state where the small amount of α_0 configuration exists.

We have also checked the stability of these states to select the candidates for the resonance states. For this purpose, we have investigated the behavior of the energy convergence with respect to the N quanta of the harmonic oscillator. We have also analyzed whether the obtained states have gaslike or linear-chain structure, and the candidate for the excited Hoyle state (2^+) was found.

Because our wave functions are constructed from purely Pauli-allowed states, the applicability for further analyses is quite large. For instance, applying non-Hermitian formalism by taking the correct boundary condition based on the complex scaling method (CSM) [28,29] is feasible. In the forthcoming paper, we will construct the formalism that can be combined with CSM. The present analysis is an important first step for the analysis along this line.

[1] K. Ikeda, N. Takigawa, and H. Horiuchi, Prog. Theor. Phys. Suppl. **Extra Number**, 464 (1968).
[2] F. Hoyle, Astrophys. J. Suppl. **1**, 121 (1954).
[3] Y. Fujiwara *et al.*, Prog. Theor. Phys. Suppl. **68**, 60 (1980).
[4] Y. Suzuki, K. Arai, Y. Ogawa, and K. Varga, Phys. Rev. C **54**, 2073 (1996).
[5] A. Tohsaki, H. Horiuchi, P. Schuck, and G. Röpke, Phys. Rev. Lett. **87**, 192501 (2001).
[6] Y. Funaki *et al.*, Eur. Phys. J. A **24**, 321 (2005).
[7] M. Chernykh, H. Feldmeier, T. Neff, P. von Neumann-Cosel, and A. Richter, Phys. Rev. Lett. **98**, 032501 (2007); T. Neff and H. Feldmeier, Few-Body Syst. **45**, 145 (2009).
[8] T. Kawabata *et al.*, Phys. Lett. B **646**, 6 (2007).
[9] Y. Sasamoto *et al.*, Mod. Phys. Lett. A **21**, 2393 (2006).
[10] T. Yoshida, N. Itagaki, and T. Otsuka, Phys. Rev. C **79**, 034308 (2009).
[11] E. Uegaki *et al.*, Prog. Theor. Phys. **62**, 1621 (1979).
[12] H. Horiuchi, Prog. Theor. Phys. Suppl. **62**, 90 (1977).
[13] T. Yamada *et al.*, Prog. Theor. Phys. **120**, 6 (2008).
[14] B. F. Bayman and A. Bohr, Nucl. Phys. **9**, 596 (1959).
[15] F. Ajzenberg-Selove and C. L. Busch, Nucl. Phys. A **336**, 1 (1980).
[16] F. Arickx, Nucl. Phys. A **268**, 347 (1976); G. Rosensteel and D. J. Rowe, Phys. Rev. Lett. **38**, 10 (1977); K. T. Hecht and D. Braunschweig, Nucl. Phys. A **295**, 34 (1978); Y. Suzuki, *ibid.* **448**, 395 (1986).
[17] F. Arickx, J. Broechove, and E. Deumens, Nucl. Phys. A **377**, 121 (1982).
[18] K. Katō and H. Tanaka, Prog. Theor. Phys. **81**, 841 (1989).

[19] K. Katō, H. Kazama, and H. Tanaka, Prog. Theor. Phys. **76**, 75 (1986).
[20] K. Katō, K. Fukatsu, and H. Tanaka, Prog. Theor. Phys. **80**, 663 (1989).
[21] S. Saitō, Prog. Theor. Phys. **41**, 705 (1969).
[22] S. Saitō, Prog. Theor. Phys. **62**, 11 (1977).
[23] K. Katō and H. Bandō, Prog. Theor. Phys. **53**, 692 (1975).
[24] H. Horiuchi, Prog. Theor. Phys. **53**, 447 (1975); **58**, 204 (1989).
[25] E. W. Schmidt and K. Wildermuth, Nucl. Phys. **26**, 463 (1961).
[26] C. Kurokawa and K. Katō, Phys. Rev. C **71**, 021301 (2005); Nucl. Phys. A **792**, 87 (2007).
[27] M. Itoh *et al.*, Nucl. Phys. A **738**, 268 (2004).
[28] J. Aguilar and J. M. Combes, Commun. Math. Phys. **22**, 269 (1971).
[29] E. Balslev and J. M. Combes, Commun. Math. Phys. **22**, 280 (1971).